Model of mode-locked quantum-well semiconductor laser based on InGaAs/InGaAlAs/InP heterostructure

D A Rybalko[1], I S Polukhin[1], Y V Solov'ev[1], G A Mikhailovskiy[1], M A Odnoblyudov[1], A.E. Gubenko[1], D.A. Livshits[1], A.N. Firsov[1], A.N. Kirsyaev[1], A.A. Efremov[1], V E Bougrov[2]
[1]Peter the Great St. Petersburg Polytechnic University, Saint Petersburg 195251, Russia
[2]ITMO University, Saint Petersburg 197101, Russia

Abstract. We propose a model for operation of mode-locked (ML) quantum-well semiconductor laser consisting of a reverse biased saturable absorber and a forward biased amplifying section. To describe the dynamics of this laser we use the traveling wave model. Numerical simulations performed for the InGaAs/InGaAlAs laser structure emitting at 1,55 um.

1. Introduction

ML semiconductor lasers could play a significant role as microwave photonic components at telecom wavelengths [1,2]. Such devices can be used for determination of a sampling rate in microwave photonic analog-to-digital converters [3]. Passive ML lasers based on semiconductors materials have many benefits in comparison with liquid organic dyes and solid crystal passive ML lasers, such a small size, a low power consumption and an ability to plug in a monolith integrated circuit. Today the passive mode-locked lasers are successfully deployed in quantum dots and wells for 1.3-1.55 μm wave length range on GaAs and InP substrates [4-6]. In this work, we consider a model of a two-section quantum-well ML laser consisting of a reverse biased saturable absorber and a forward biased amplifying (gain) section. We perform a comprehensive numerical study of the operation regimes of this laser and estimate main characteristics of ML pulses such as the repetition rate, width and shape of the pulse depending on parameters of laser structure. One of the most important parts of the ML model is a function of the spontaneous noise, which affects the initial emission, width of the pulse and the time jitter. In our model, we propose to use the Rayleigh distribution to describe the spontaneous processes. The numerical calculations performed for the novel laser structure emitting at 1.55 um wavelength based on InGaAs/InGaAlAs quantum well structure grown on InP substrate.

2. Model

This model allows to define the main laser specifications, such as pulse repetition rate, pulse shape/width and power. Passive mode-locking models can be divided into two groups as follows: electromagnetic field equation depending on time and electromagnetic field equation depending on frequency [7-9]. Models with frequency-based equations can be advantageous in terms of time for numerical calculations [7]. In this model, we consider the spatio-temporal evolution of the two counter-propagating optical fields $E^+(z,t)$ and $E^-(z,t)$ and carrier density $n(z,t)$. After fixing wavelength λ_0, the field in the laser cavity can be represented as a superposition of two slowly varying complex amplitudes ($\left|\frac{1}{E^\pm}\frac{\partial E^\pm}{\partial z}\right| \ll k_0$, $\left|\frac{1}{E^\pm}\frac{\partial E^\pm}{\partial z}\right| \ll \omega_0$) $E^+(z,t)$ and $E^-(z,t)$ of forward and backward propagating waves. Here, t denotes time and z is the coordinate along the cavity axis ($0<z<L$), k_0 is wave vector, ω_0 is carrier wave frequency. The amplitudes $E^\pm(z, t)$ of the two waves counter-propagating in the cavity satisfy the traveling wave equations:

$$\frac{\partial E^+}{\partial t} + v_g \frac{\partial E^+}{\partial z} = v_g \frac{\Gamma\sigma(n-n_t)}{2}(1 - i\alpha_H)E^+ + \Gamma\frac{v_g\sigma n_t}{2{\omega_g}^2} - v_g\frac{\alpha_i}{2}E^+ + F_{sp}^+ , \quad (1)$$

$$\frac{\partial E^-}{\partial t} - v_g \frac{\partial E^-}{\partial z} = v_g \frac{\Gamma\sigma(n-n_t)}{2}(1 - i\alpha_H)E^- + \Gamma\frac{v_g\sigma n_t}{2{\omega_g}^2} - v_g\frac{\alpha_i}{2}E^- + F_{sp}^- , \quad (2)$$

where v_g is group velocity, σ is differential amplification in the gain section or absorption in the saturable absorber, n is the carrier concentration in the quantum-well ground state, n_t is transparency concentration, α_H is the Henry-factor, α_i is the internal loss, Γ is the optical confinement factor, ω_g is the frequency dispersion coefficient, F_{sp} is the spontaneous emission noise. The measurement unit of the field amplitude is chosen so that the sum $\left|E^+\right|^2 + \left|E^-\right|^2$ corresponds to the local photons concentration. The rate equation in this system is

$$\frac{\partial n}{\partial t} = \frac{I(z)}{eV} - R - v_g\sigma(n - n_t)(|E^+|^2 + |E^-|^2) , \quad (3)$$

where e is the elementary charge, $I(z)$ is the injection current. $I(z)$=0 in the saturable absorber and $I(z)=I_G$ in the gain section. V is volume of active area, R described all recombination mechanisms in structure. For absorber section we consider R as:

(4)

where D is the absorber saturation rate. For amplifier section R was:

(5)

where A is the nonradiative recombination coefficient, B is the radiative recombination coefficient, C is the Auger recombination coefficient. Boundary and initial condition for (1)-(3):

$$E^+(0,t) = r_L E^-(0,t); E^-(L,t) = r_0 E^+(L,t);$$
$$E^+(z,0) = E^-(z,0); \frac{\partial E^{\pm}(z,0)}{\partial t} = 0; \quad (6)$$
$$n(z,0) = n_t ,$$

where $r_{0,L}$ are factors describing a reflectivity of the laser facets. Equations (1)-(3) with the initial and boundary conditions (6) make a closed equation system that enables to determine repetition rate, as well as width and shape of the pulse. The structure considered in this model consisted of five InGaAs/InGaAlAs quantum wells on InP substrate. The structure parameters present in table 1.

Table 1. Simulated structure parameters

No.	Parameter name	Symbol	Value	Unit
1	Group velocity	v_g	0,91 10^{10}	cm/s
2	Resonator overall length	L	0.455	cm
3	Absorber length	l_a	0.0455	cm
4	Internal loss rate	α_i	5	cm^{-1}
5	Optical confinement factor	Γ	0.025	
6	Differential gain	σ_g	4 10^{-16}	cm^2
7	Differential absorption	σ_a	2 10^{-15}	cm^2
8	Henry-factor [10]	α_H	2	
9	Transparency threshold concentration	n_t	10^{18}	cm^{-3}
10	Frequency gain dispersion rate	ω_g	7.5 10^{13}	s^{-1}
11	Nonradiative recombination coefficient [11]	A	2 10^8	s^{-1}
12	Radiative recombination coefficient [11]	B	0.96 10^{-10}	cm^3/s

13	Auger recombination coefficient [11]	C	$7\ 10^{-29}$	cm^6/s
14	Absorber relaxation rate	D	10^{11}	s^{-1}
15	Active region volume	V	$1.7\ 10^{-10}$	cm^{-3}
16	Waveguide spontaneous emission contribution [12]	β_{sp}	10^{-4}	
17	Amplitude reflection coefficient at 0 boundary	r_0	1	
18	Aamplitude reflection coefficient at L-boundary	r_L	0.9	
19	Pumping current	I_G	300-900	mA

The output power can be calculated using the following formula:

$$Power[W] = \hbar w_0 \left|E^+\right|^2 v_g \frac{V}{L \cdot \Gamma}(1 - R_L), \quad (7)$$

where $\hbar$ – the Planck constant, R_L – reflection factor of one of the mirrors.

3. Experimental Results and Discussion

The dynamics of the transition to the operation regime for a simulated laser was acquired. Transition to the one pulse generation mode is possible for parameters listed in the table and provided the voltage at the absorber is more than 4V. Figure 1 shows the result. At the initial moment of time there is the generation of multiple longitudinal modes in the amplifier area (figure 1a). Their intensity is not sufficient to illuminate the absorber, but they gradually start its saturation. Further, there is mode discrimination when the weakest modes are attenuated and the strong modes start coming to the absorber simultaneously with each other (figure 1b, c). As a result by the moment of time of 30 ns modes are locked and there is only one large pulse left. With voltage at the absorber of less than 2V the situation is slightly different. Thus, by the moment of time of 30 ns, there are two pulses instead of a single one formed in the resonator which are rather powerful to pass through the saturable absorber (figure 2b). The mechanism of ultrafast pulse formation is very sensitive to laser initial conditions. In case of low losses in resonator, the two or more pulses can be obtained. A similar result was shown in the work [12,13].

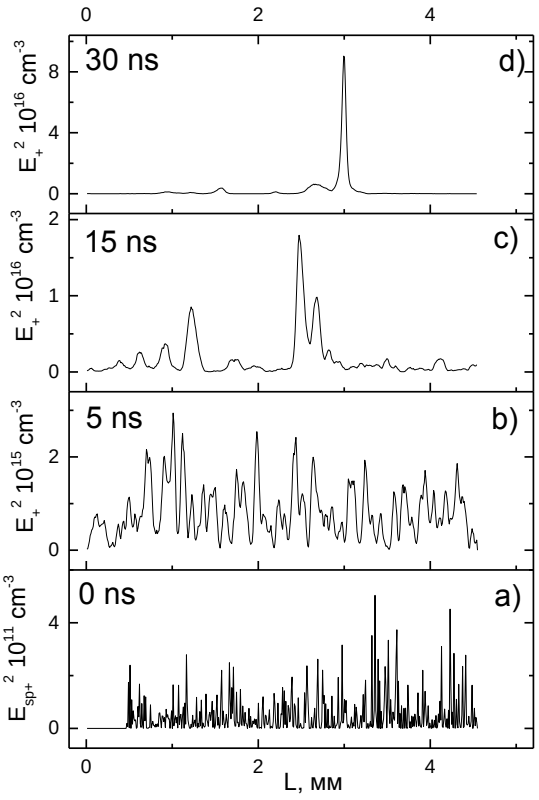

Figure 1. Distribution of radiation intensity along the laser resonator in second harmonic mode-locking.

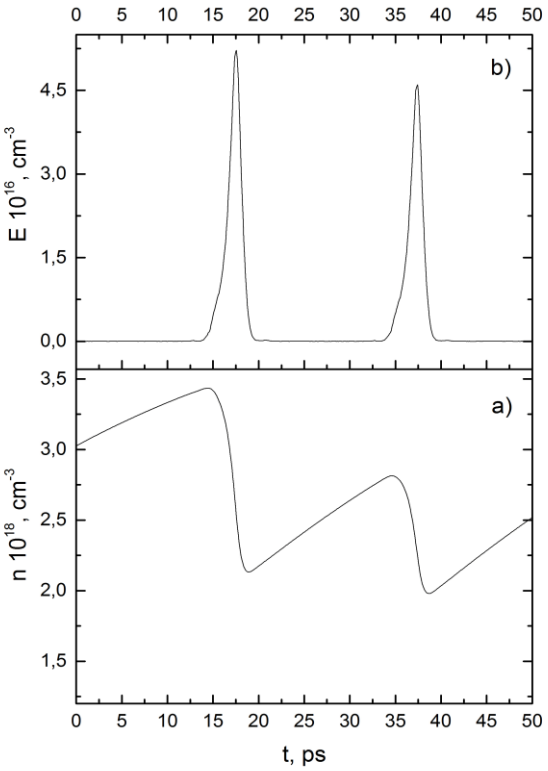

Figure 2. Changes in concentration of electrons and photons in the resonator depending on a time

The model provides an opportunity to track the changes in the concentration of both photons and electrons. Figure 2a shows the dependence of the electrons concentration on a coordinate. One can see that maximum concentration is about to coincide with the pulse shown in the figure 2b. After the pulse has passed, the electron concentration decreases which corresponds to the radiating interband transitions of electrons.

We have also investigated the influence of absorber section length on the formation of ultra-short pulses. Figure 3 shows the results. With reduction of the absorber length absorption in the resonator decreases and spurious pulses occur. Application of a laser with such radiation regime poses some difficulties: pulses have relatively small power, their position in time regarding one another may vary. Accordingly, generation of spurious pulses can be regarded as a negative process while the construction with such kind of operation is deemed as non-optimal one. Increase of absorber length is accompanied by increased losses in the resonator. This fact adds up to the mode discrimination and allows to cut off spurious modes. As a result a single pulse is formed (figure 3d, e). Optimum is found with absorber length equal to 14% of resonator length (637 μm). With further increase in absorber length no transition to mode-locking occurs since dramatically increased losses do not allow any mode amplification. One should note that these results are valid for the system with specific parameters, the optimal length of the absorbing section will be different provided the different voltage value at the absorber, as well as gain and absorption value of the medium.

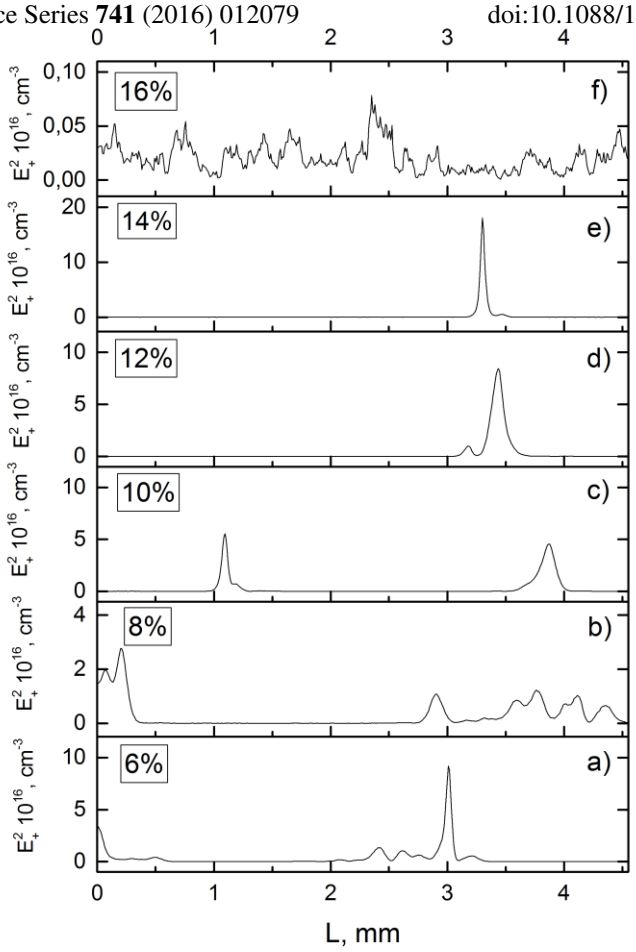

Figure 3. Intensity distribution in the resonator for different lengths of the absorber.

4. Conclusion

Represented model allows to perform numerical simulation of processes in the resonator of the semiconductor laser on quantum structures with passive mode-locking. We have received pulses of 2 ps long and 10 HHz repetition frequency for a structure with four InGaAs/InGaAlAs quantum wells and the resonator length equal to 4.55 mm. Power of the received pulses was 9.4 mW. Varying the length of the absorber has shown that the simulation predicts the possibility of optimizing laser geometric dimensions for the most effective transition to the passive mode locking. In this case the optimal length was equal to 637 μm. Further we plan to include the refractive index in the dispersion model, the effect of gain saturation and nonlinear coherent effects.

Acknowledgments

This work supported by the Ministry of Education and Science of the Russian Federation as a part of federal purpose-oriented program “Researches and development works on priority direction of Russian scientific and technological complex for 2014-2020 years”, code number 2015-14-579-0015, agreement № 14.578.21.0100, unique identifier RFMEFI57814X0100.

References

[1] G.C. Valley, Optics Express, **15** (2007), p. 1955.
[2] A. Khilo, S.J. Spector, E. Matthew, et. al., Optics Express, **20** (2012), p. 4454
[3] R.S. Staricov, Uspekhi sovremennoi radioelektroniki (in Russian). **2** (2015), p. 3.
[4] K. Merghem, A. Akrout, A. Martinez et al., Optics Express, **16** 14 (2008) p. 10675
[5] Xiaodong Huang, A. Stintz, Hua Li, Appl. Phys. Lett. **78**, 2825 (2001) p. 2825.
[6] R. Rosales, K. Merghem, A. Martinez, IEEE Journal of Selected Topics in Quantum Electronics, **17**, 5, (2011), p. 1292
[7] E.A Avrutin, J.H. Marsh, E.L. Portnoi, Proceedings-Optoelectronics, **147** (2000), p. 251.
[8] M. Radziunas, A. G. Vladimirov, E.A. Viktorov et al., J. of Quant. El., **47** (2011), p. 935.
[9] A. G. Vladimirov, D. Turaev, Physical Review A **72** (2005), p. 033808.
[10] G.A. Mikhailovskiy, I.S. Polukhin, D.A. Rybalko et. al., Tech. Ph. Lett., vol **42** (2016)
[11] A. Fali, E. Rajaei, and Z. Kaftroudi, J. of the Korean Physical Society, **64** (2014), p. 16.
[12] M. Radziunas, A. G. Vladimirov and E. A. Viktorov, Proceedings of SPIE, **7720** (2010), p. 77200X-1.
[13] A. G. Vladimirov, D. Turaev, Physical Review A **72**, 033808 2005